

## Convection in binary mixtures: A Galerkin model with impermeable boundary conditions

S. J. Linz and M. Lücke

*Institut für Theoretische Physik, Universität des Saarlandes, D-6600 Saarbrücken, West Germany*

(Received 1 December 1986)

We derive an eight-mode model with horizontal boundaries that are impermeable to the concentration current and free slip for the velocity. Its properties are elucidated and compared with theoretical results obtained for other boundaries. Impermeable boundaries cause an additional coupling between temperature and concentration gradients which significantly changes linear and nonlinear properties as compared to those of permeable boundaries.

Binary fluid mixtures heated from below display,<sup>1-5</sup> close to onset of convection, interesting behavior caused by interacting momentum, heat, and concentration currents. Except for stability analyses<sup>6,7</sup> of the conductive state done for no-slip impermeable (NSI) boundary conditions all theoretical<sup>8-12</sup> work uses free-slip permeable (FSP) conditions. These approaches ignore the coupling between convective temperature and concentration gradients that arises when the vertical concentration current which is a weighted sum of these gradients is forced to zero at an impermeable horizontal boundary. Its effect is studied here with a Galerkin approximation. Since such models<sup>13</sup> for one-component fluids do not depend much on the slip properties of the boundaries we consider here for convenience free-slip impermeable (FSI) horizontal boundaries.

To describe small-amplitude Soret-driven convective flow in the form of straight rolls seen in experiments<sup>3,5</sup> we truncate the spatial mode expansion appropriate to FSI conditions:

$$w(x, z; t) = [w_{11}(t)e^{-ikx} + \text{c.c.}] \sqrt{2} \sin(\pi z), \quad (1a)$$

$$\theta(x, z; t) = [\theta_{11}(t)e^{-ikx} + \text{c.c.}] \times \sqrt{2} \sin(\pi z) + \theta_{02}(t) \sqrt{2} \sin(2\pi z), \quad (1b)$$

$$\zeta(x, z; t) = [\zeta_{10}(t)e^{-ikx} + \text{c.c.}] + \zeta_{01}(t) \sqrt{2} \cos(\pi z). \quad (1c)$$

Here  $w$  is the vertical velocity and  $\theta$  the deviation from the conductive temperature profile. Instead of the convective concentration  $c(x, z; t)$  we use the field  $\zeta = c - \psi\theta$  with an expansion of its  $z$  dependence in terms of  $\cos(n\pi z)$ . Of course the truncation (1) is inadequate for localized convective states.<sup>3,5</sup> Since  $\zeta_{11}$  and  $\zeta_{02}$  do not drive the modes in (1) they are not considered here. The critical modes  $w_{11}$ ,  $\theta_{11}$ , and  $\zeta_{10}$  excite via nonlinearities the current-carrying modes  $\theta_{02}$  and  $\zeta_{01}$ . The mode  $\theta_{01}$  is damped away.

Note that (1c) guarantees impermeability of the horizontal boundaries at  $z=0, 1$  since the vertical component of the diffusive concentration current,  $\mathbf{j}_c = -L\nabla\zeta$ , vanishes there. For finite Lewis number  $L$  this constraint causes additional coupling between concentration and temperature.

We have scaled length by the layer thickness  $d$ , time by  $d^2/\kappa$  where  $\kappa$  is the thermal diffusivity, temperature by  $\nu\kappa/\beta_1gd^3$ , and concentration by  $\nu\kappa/\beta_2gd^3$ . Here  $\nu$  is the

kinematic viscosity,  $g$  the gravitational acceleration,  $\beta_1$  ( $\beta_2$ ) the thermal (solutal) expansion coefficient at constant concentration (temperature) and pressure, and  $\psi$  the separation ratio.<sup>9</sup>

Since the horizontal variation of the fields is given by  $A(t)e^{-ikx} + \text{c.c.}$  the convective roll pattern of amplitude  $|A(t)|$  is standing if  $|\phi(t)| = \text{const}$  where  $\phi(t)$  is the phase of  $A$ . For  $\phi(t) = \omega t$  a pattern of amplitude  $|A(t)|$  propagates with constant speed  $\dot{\phi}/k$ . The general spatiotemporal behavior of  $|A(t)| \cos[kx - \phi(t)]$  can be more complicated.

Projecting the standard Oberbeck-Boussinesq equations<sup>9</sup> (without Dufour effect) onto the eight modes retained in (1) one obtains a generalized Lorenz model

$$\tau \dot{\mathbf{X}}(t) = -\sigma \hat{q}^2 \mathbf{X}(t) + \sigma \frac{\hat{k}^2}{\hat{q}^2} \left[ (1 + \psi) \mathbf{Y}(t) + \frac{8}{\pi^2} \mathbf{U}(t) \right], \quad (2a)$$

$$\tau \dot{\mathbf{Y}}(t) = -\hat{q}^2 \mathbf{Y}(t) + [r - Z(t)] \mathbf{X}(t), \quad (2b)$$

$$\tau \dot{Z}(t) = -b [Z(t) - \mathbf{X}(t) \cdot \mathbf{Y}(t)], \quad (2c)$$

$$\tau \dot{\mathbf{U}}(t) = -\frac{L}{3} \hat{k}^2 \mathbf{U}(t) + \hat{q}^2 \psi \mathbf{Y}(t) + V(t) \mathbf{X}(t), \quad (2d)$$

$$\tau \dot{V}(t) = -b \left[ \frac{1}{2} \mathbf{X}(t) \cdot \mathbf{U}(t) + \frac{2}{3} \psi Z(t) + (L/4) V(t) \right]. \quad (2e)$$

Here the critical modes

$$\mathbf{X} = (X_1, X_2) = (1/q_c^0) (\text{Re} w_{11}, \text{Im} w_{11}), \quad (3a)$$

$$\mathbf{Y} = (Y_1, Y_2) = (q_c^0/R_c^0) (\text{Re} \theta_{11}, \text{Im} \theta_{11}), \quad (3b)$$

$$\mathbf{U} = (U_1, U_2) = (\pi q_c^0/2\sqrt{2}R_c^0) (\text{Re} \zeta_{10}, \text{Im} \zeta_{10}) \quad (3c)$$

are combined into two-component vectors. The current-carrying modes

$$Z = (-\pi\sqrt{2}/R_c^0) \theta_{02}, \quad V = (\pi^2/2\sqrt{2}R_c^0) \zeta_{01} \quad (3d)$$

are scalars in this notation. The constants  $(k_c^0)^2 = \pi^2/2$ ,  $(q_c^0)^2 = (k_c^0)^2 + \pi^2$ ,  $R_c^0 = (q_c^0)^6/(k_c^0)^2$ ,  $\tau = 1/(q_c^0)^2$ , and  $b = 4\pi^2/(q_c^0)^2$  are critical quantities at  $\psi=0$ , and  $\sigma$  is the Prandtl number. We reduced the Rayleigh number  $R$  and the wave number  $k$  by

$$r = R/R_c^0, \quad \hat{k} = k/k_c^0, \quad \hat{q}^2 = (k^2 + \pi^2)/(q_c^0)^2. \quad (3e)$$

With the truncation (1) the Nusselt number is given by

$$N(t) = 1 + 2Z(t)/r. \quad (4)$$

The system (2) looks similar to the FSP model.<sup>11,12</sup> However, the differences, e.g., in the  $\mathbf{U}$  equation, are significant. Moreover,  $\mathbf{U}$  and  $V$  are here modes of the field  $\zeta$ . Setting  $X_2=Y_2=U_2=0$  yields a five-mode model which allows only standing patterns. Like the FSP model<sup>11,12</sup> the system (2) is invariant against simultaneously rotating or inverting the vectors  $\mathbf{X}, \mathbf{Y}, \mathbf{U}$  which reflects the invariance of the convective pattern (1) against horizontal translation or reflections at the plane  $x=0$ . Thus properties<sup>12</sup> caused by these symmetries<sup>8</sup> show up here as well.

The conductive state, i.e., the zero state of (2) loses stability against monotonous growth of a roll pattern of wave number  $\hat{k}$  with a degenerate pair of real eigenvalues becoming positive at

$$r_{\text{stat}}(\hat{k}) = (\hat{q}^6/\hat{k}^2)[1 + \psi + (\psi/\hat{L})(8/\pi^2)]^{-1}, \quad (5)$$

if  $\psi$  is bigger than the polycritical value

$$\psi_{\text{pc}}(\hat{k}) = -(1 + \sigma)[1 + \sigma + (1 + \sigma)(8/\pi^2\hat{L})\sigma(8/\pi^2\hat{L}^2)]^{-1}. \quad (6)$$

Here  $\hat{L} = (\hat{k}^2/3\hat{q}^2)L$ .

The critical wave number of (5) vanishes for  $\psi \geq \psi_0 = L(16/\pi^2 - L)^{-1}$  and is given for  $\psi \leq \psi_0$  by

$$(\hat{k}_{\text{stat}}^c)^2 = [(1 + \psi)L - (16/\pi^2)\psi] \times [(1 + \psi)L + (8/\pi^2)\psi]^{-1}. \quad (7)$$

In Fig. 1 we compare  $(\hat{k}_{\text{stat}}^c)^2$  and the critical Rayleigh number  $r_{\text{stat}}^c$  with a one-mode NSI variational result.<sup>6</sup> We also compare our  $r_{\text{stat}}(\hat{k})$  at  $\psi = \psi_0$  with the NSI result<sup>6</sup> and the FSP boundary<sup>9</sup>  $(\hat{q}^6/\hat{k}^2)(1 + \psi + \psi/L)^{-1}$  which diverges for  $\hat{k} \rightarrow 0$  in contrast to the two impermeable results. Since the latter two are similar to each other the slip condition is less influential than the boundary condition on the concentration current.

A Hopf bifurcation occurs at

$$r_{\text{osc}}(\hat{k}) = (\hat{q}^6/\hat{k}^2)(1 + \sigma)(1 + \hat{L})(1 + \hat{L}/\sigma) \times [1 + \sigma + \psi(1 + \sigma - 8/\pi^2)]^{-1}. \quad (8)$$

There two degenerate pairs of complex conjugate eigenvalues cross the imaginary axis with a frequency  $\omega$  given by

$$\omega^2 \tau^2 / \hat{q}^4 = -\hat{L}^2 - (8/\pi^2)\psi(1 + \hat{L})(\sigma + \hat{L}) \times [1 + \sigma + \psi(1 + \sigma - 8/\pi^2)]^{-1}, \quad (9)$$

as long as  $\psi < \psi_{\text{pc}}(\hat{k})$ . At  $\psi_{\text{pc}}(\hat{k})$  [Eq. (6)], i.e., the intersection of  $r_{\text{osc}}(\hat{k})$  and  $r_{\text{stat}}(\hat{k})$  the frequency vanishes such that four eigenvalues are simultaneously zero. The wave-number dependence of  $r_{\text{osc}}(\hat{k})$  [Eq. (8)] is for not too large  $|\psi|$  very similar to the NSI<sup>6</sup> and FSP<sup>9</sup> result.

The critical wave number of (8) is for small  $L$  given by

$$(\hat{k}_{\text{osc}}^c)^2 = 1 - [(1 + \sigma)/(3\sigma)]L + O(L^2).$$

In Fig. 2 we compare our *critical curves*  $r_{\text{stat}}^c$  and  $r_{\text{osc}}^c$  in the  $r - \psi$  plane in the vicinity of their intersection with NSI<sup>6</sup> and FSP<sup>9</sup> results. For both impermeable conditions, FSI and NSI (Refs. 6 and 7),  $k_{\text{stat}}^c \neq k_{\text{osc}}^c$  at this intersection point so that two spatially different convective

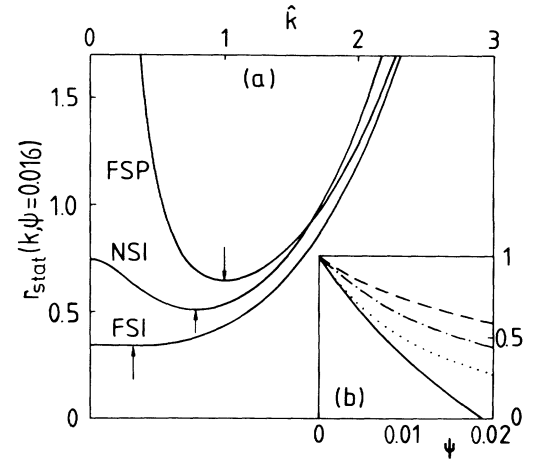


FIG. 1. (a) Stability curves  $r_{\text{stat}}(\hat{k})$  for  $\psi=0.016$ ,  $L=0.03$ ,  $\sigma=0.6$ . Boundary conditions are FSI (our result), NSI (Ref. 6), and FSP (Ref. 9). Arrows mark the critical values. (b)  $\psi$  dependence of  $(\hat{k}_{\text{stat}}^c)^2$  (FSI, solid curve; NSI, dashed curve), and of  $r_{\text{stat}}^c$  (FSI, dotted curve; NSI, dash-dotted curve).

structures with wave numbers differing by a few percent [cf. Fig. 2(b)] can grow there. That might cause interesting spatiotemporal behavior. Furthermore, at this intersection of  $r_{\text{stat}}^c$  and  $r_{\text{osc}}^c$  the Hopf frequency although being small is nonzero. The two convective states which can grow there are structurally and dynamically distinct. This degeneracy of the codimension-two point of the permeable system is lifted by impermeable boundaries. Only where  $r_{\text{stat}}(\hat{k})$  and  $r_{\text{osc}}(\hat{k})$  intersect with a *common* fixed  $\hat{k}$  [cf. Fig. 2(b)] does  $\omega$  vanish. Thus the stability behavior of the conductive state depends for  $\psi \geq 0$  sensitively on the boundary condition of the concentration flux.

We now address the nonlinear properties of our model.

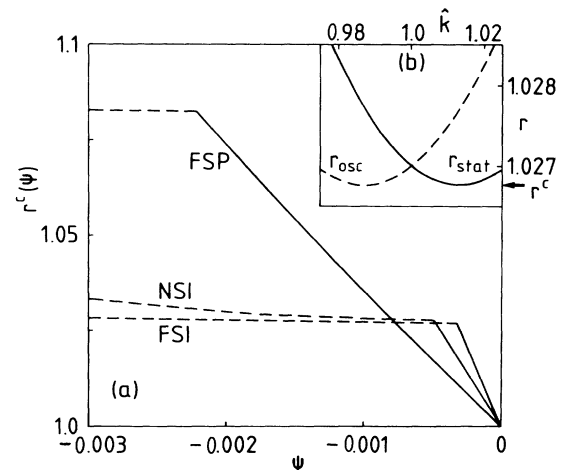


FIG. 2. (a) Stability boundaries of the conductive state,  $r_{\text{osc}}^c$  (dashed lines) and  $r_{\text{stat}}^c$  (solid lines). Parameters as in Fig. 1. (b) Stability curves  $r_{\text{osc}}^c(\hat{k})$  (dashed line) and  $r_{\text{stat}}^c(\hat{k})$  (solid line) of our FSI model for  $\psi = -3.205 \times 10^{-4}$  where  $r_{\text{osc}}^c = r_{\text{stat}}^c$ .

Its fixed points are given by

$$\hat{q}^2 N_1 N_2 (X^4 + \alpha X^2 + \beta) \mathbf{X} = 0, \quad (10a)$$

$$\mathbf{Y} = r N_1 \mathbf{X}, \quad \mathbf{U} = r \psi [(L/2) \hat{q}^2 - \frac{4}{3} X^2] N_1 N_2 \mathbf{X}, \quad (10b)$$

$$Z = r N_1 X^2, \quad V = -r \psi (\hat{q}^2 + \frac{4}{3} \hat{k}^2 L) N_1 N_2 X^2, \quad (10c)$$

$$N_1 = (\hat{q}^2 + X^2)^{-1}, \quad N_2 = (\frac{1}{6} \hat{k}^2 L^2 + X^2)^{-1}, \quad (10d)$$

$$\alpha = \hat{q}^2 + (L^2/6) \hat{k}^2 - (\hat{k}^2/\hat{q}^4) r [1 + \psi - (32/3\pi^2) \psi], \quad (10e)$$

$$\beta = (\hat{k}^2/6\hat{q}^4) L^2 [\hat{q}^6 - \hat{k}^2 r (1 + \psi)] - 4 L r \psi (\hat{k}^2/\hat{q}^2 \pi^2). \quad (10f)$$

As in the FSP model<sup>12</sup> there is a continuous family of convective fixed points with  $\mathbf{X}, \mathbf{Y}, \mathbf{U}$  being nonzero and collinear. Without symmetry-breaking perturbations the initial conditions select the common direction of these vectors, i.e., the final phase of the convective pattern. Had we added an inhomogeneity<sup>12</sup>  $\sigma \hat{q}^2 \xi$  in (2a) the right-hand side of (10a) would be  $\xi$ , thereby selecting<sup>12</sup> the fixed-point phase.

The bifurcation to stationary convection is forwards for

$$\psi > \psi_t = - \left[ 1 + \frac{8}{9\pi^2 \hat{L}} \left( \frac{6}{\hat{L}^2} + \frac{8}{\hat{L}} + 9 \frac{\hat{q}^2}{\hat{k}^2} \right) \frac{\hat{k}^2}{\hat{q}^2} \right]^{-1}, \quad (11)$$

tricritical at  $\psi_t$ , and backwards for  $\psi < \psi_t < 0$  with a saddle node located where  $\alpha^2 = 4\beta$ .

Before we discuss the dynamics of (2) note that including into the FSP five-mode model the modes  $X_2, Y_2, U_2$  that are required by symmetry renders the upper branch of overturning convection at  $\psi < \psi_t$  unstable for  $r < r_{\text{FSP}}^c = r_{\text{osc}}^c$ .<sup>11,12</sup> There one real eigenvalue becomes positive.<sup>12</sup> In our FSI model the situation is different (cf. Fig. 3): The overturning branch is stable (unstable) for small (large)  $r$ . The instability occurs at  $r'(\psi) > r_{\text{osc}}^c$  via a Hopf bifurcation involving *one* complex conjugate pair of eigenvalues. The location  $r'(\psi)$  varies strongly with  $\psi$ ,

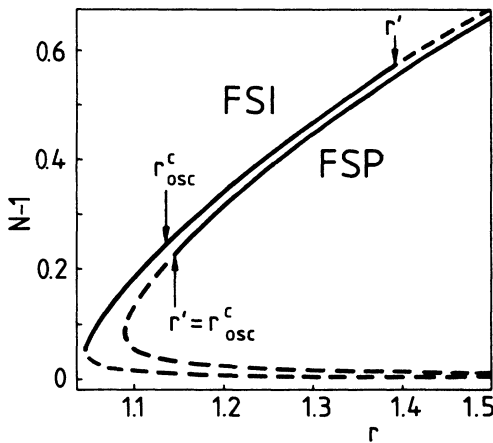


FIG. 3. Nusselt number for steady overturning convection in the eight-mode FSI and FSP (Refs. 11 and 12) models for  $\psi = -0.12$ ,  $L = 0.015$ ,  $\sigma = 18.4$ . Stable branches are shown by full lines, unstable ones by dashed lines. The instabilities at  $r'$  are explained in the text. The Hopf bifurcation of the *conductive* state occurs at  $r_{\text{osc}}^c$ .

e.g.,  $r'(\psi \rightarrow 0)$  connects to the Hopf bifurcation of the standard Lorenz model<sup>14</sup> at large  $r$ . The bifurcation at  $r'(\psi)$  is also present in the five-mode version ( $X_2 = Y_2 = U_2 = 0$ ) of our model. Thus at  $r'(\psi)$  a nonlinear standing-wave (SW) solution bifurcates:  $\mathbf{X}, \mathbf{Y}, \mathbf{U}$  oscillate collinearly around the unstable overturning convection fixed point with a frequency  $\omega'$  given by the imaginary part of the eigenvalue pair describing this instability. We have checked for a few  $L, \sigma, \psi$  that *immediately* above  $r'(\psi)$  the system runs into a nonlinear SW limit cycle.

For larger  $r$ , however, a modulated-traveling-wave (MTW) solution is selected at *large* times unless one chooses special initial conditions, e.g.,  $\mathbf{X}, \mathbf{Y}, \mathbf{U}$  collinear (then also  $\dot{\mathbf{X}}, \dot{\mathbf{Y}}, \dot{\mathbf{U}}$  are collinear so that the phase cannot change). In Fig. 4 we show a stationary MTW at  $r = 1.05r'$  in the  $(X_1, X_2)$  plane. Therein, the field amplitudes  $X$  and  $Y$  of  $w$  and  $\theta$  oscillate around the unstable fixed-point circle of overturning convection with a frequency  $\omega_A = 10.89$  that is 4.6% smaller than  $\omega'$ . The Nusselt number (4) basically being determined by  $X^2$  oscillates twice as fast. There is a small phase difference of about  $0.01\pi$  between  $\mathbf{X}$  and  $\mathbf{Y}$ . The phase velocity  $\dot{\phi}$  of  $\mathbf{X}$ , and similarly of  $\mathbf{Y}$ , i.e., the propagation speed  $\dot{\phi}/k$  of the MTW is *not* constant:  $\dot{\phi}$  oscillates with frequency  $\omega_A$  and amplitude 0.12 around the mean  $\langle \dot{\phi} \rangle = 0.413$  which is close to the difference  $\omega' - \omega_A = 0.53$ . Furthermore,  $\langle \dot{\phi} \rangle$  seems to be incommensurate with the amplitude oscillation. The oscillations of  $\mathbf{U}$ , i.e., of the fields  $\zeta$  and  $c$  are slightly more complicated than those of  $\mathbf{X}$  and  $\mathbf{Y}$ .

For  $r > r_{\text{osc}}^c$  the transient growth behavior out of the conductive state is similar to that of the FSP model.<sup>12</sup> For special initial conditions a standing wave,  $\mathbf{X} = \mathbf{X}_0 e^{i\omega t} \times \cos(\omega t)$ , or a traveling wave grows with

$$\mathbf{X} = (X_1, X_2) \sim e^{i\omega t} (\cos \omega t, \sin \omega t)$$

rotating on a circular spiral. Typical initial conditions,

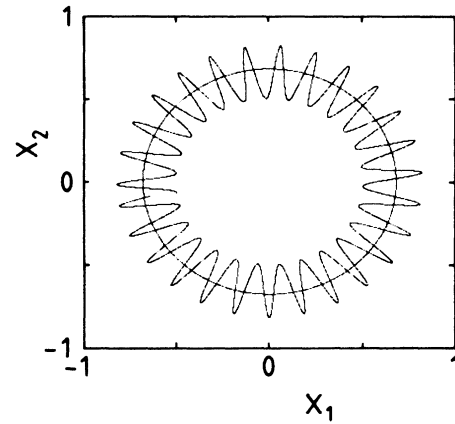


FIG. 4. Stationary MTW solution in the  $X_1, X_2$  plane for a time interval of 15.75 ( $\psi, L, \sigma$  as in Fig. 3,  $r = 1.05$ ,  $r' \approx 1.452$ ). Stationarity is not reached before 150 diffusion times. The circle shows the unstable fixed points of overturning convection. The oscillation frequency of amplitude  $X$  and phase velocity  $\dot{\phi}$  is  $\omega_A = 10.89$ . The mean rotation rate  $\langle \dot{\phi} \rangle \approx 0.413$  seems to be incommensurate with  $\omega_A$ .

however, lead to a MTW where  $\mathbf{X}$  rotates outwards on elliptic spirals around the origin. Its initial rotation period is given by the Hopf frequency  $\omega$  [Eq. (9)] and the growth rate  $\gamma$  is determined by the corresponding real part. The elliptic motion causes a  $2\omega$  oscillation of  $X$  and of the Nusselt number. Also the phase velocity  $\dot{\phi}$  oscillates with  $2\omega$  around  $\langle \dot{\phi} \rangle = \omega$ . At longer times  $\dot{\phi}$  decreases<sup>12</sup> and goes to zero when approaching the stable overturning con-

vective fixed point at  $r < r'$  or the SW limit cycle immediately above  $r'$ . Also when the final state is a MTW as in Fig. 4 the phase velocity first decreases almost to zero. But it grows again and approaches in an oscillatory fashion its final-limit cycle dynamics.

This work was supported by Deutsche Forschungsgemeinschaft.

<sup>1</sup>For a review, see, for instance, J. K. Platten and J. C. Legros, *Convection in Liquids* (Springer, Berlin, 1984).

<sup>2</sup>G. Ahlers and I. Rehberg, *Phys. Rev. Lett.* **56**, 1373 (1986), and previous work cited therein; H. Gao and R. P. Behringer, *Phys. Rev. A* **34**, 697 (1986).

<sup>3</sup>P. Kolodner, A. Passner, C. M. Surko, and R. W. Walden, *Phys. Rev. Lett.* **56**, 2621 (1986), and previous work cited therein.

<sup>4</sup>E. Moses and V. Steinberg, *Phys. Rev. A* **34**, 693 (1986); *Phys. Rev. Lett.* **57**, 2018 (1986).

<sup>5</sup>R. Heinrichs, G. Ahlers, and D. S. Cannell (unpublished).

<sup>6</sup>D. T. J. Hurle and E. Jakeman, *J. Fluid Mech.* **47**, 667 (1971).

<sup>7</sup>D. Gutkowicz-Krusin, M. A. Collins, and J. Ross, *Phys. Fluids* **22**, 1443 (1979); **22**, 1451 (1979).

<sup>8</sup>E. Knobloch, *Phys. Rev. A* **34**, 1538 (1986), and work cited therein.

<sup>9</sup>H. Brand, P. C. Hohenberg, and V. Steinberg, *Phys. Rev. A* **30**, 2548 (1984).

<sup>10</sup>G. Veronis, *J. Mar. Res.* **23**, 1 (1965); J. K. Platten and G. Chavepeyer, *Int. J. Heat Mass Transfer* **18**, 1071 (1975); L. N. Da Costa, E. Knobloch, and N. O. Weiss, *J. Fluid Mech.* **109**, 25 (1981).

<sup>11</sup>M. C. Cross, *Phys. Lett.* **119A**, 21 (1986).

<sup>12</sup>G. Ahlers and M. Lücke, *Phys. Rev. A* **35**, 470 (1987).

<sup>13</sup>G. Ahlers, P. C. Hohenberg, and M. Lücke, *Phys. Rev. A* **32**, 3493 (1985); J. Niederländer, diploma thesis, Universität Saarbrücken, 1986 (unpublished).

<sup>14</sup>E. N. Lorenz, *J. Atmos. Sci.* **20**, 130 (1963).